Proceedings of the 2nd Croatian Conference on Earthquake Engineering - 2CroCEE
Zagreb, Croatia - March 22 to 24, 2023

DOI: https://doi.org/10.5592/CO/2CroCEE.2023.122

EXPERIMENTAL AND NUMERICAL IN-PLANE SEISMIC BEHAVIOUR OF AN INNOVATIVE STEEL REINFORCEMENT SYSTEM FOR URM WALLS

Luca Albanesi [(1)], Nicolò Damiani [(2)], Carlo Filippo Manzini [(3)], Paolo Morandi [(4)]

[(1)] *Department of Construction and Infrastructure - EUCENTRE Foundation, Pavia, Italy, luca.albanesi@eucentre.it*
[(2)] *UME Graduate School, IUSS Pavia, Pavia, Italy, nicolo.damiani@iusspavia.it*
[(3)] *Department of Construction and Infrastructure - EUCENTRE Foundation, Pavia, Italy, carlo.manzini@eucentre.it*
[(4)] *Department of Construction and Infrastructure - EUCENTRE Foundation, Pavia, Italy, paolo.morandi@eucentre.it*

Abstract

An experimental campaign, followed by a numerical research, aimed at evaluating the in-plane seismic behaviour of an innovative steel modular system (named "Resisto 5.9", designed by Progetto Sisma s.r.l.) for the reinforcement of load-bearing masonry walls, has been performed at the EUCENTRE Foundation in Pavia. Different masonry typologies, selected among the most common solutions in Italian existing buildings, were considered in this study. In this paper, the results related to a solid clay bricks masonry, assembled using lime mortar in "header bond" pattern, are reported. A complete mechanical characterization of units, mortars, masonry typologies and of the strengthening system components (*i.e.* steel elements and anchors) has been carried out. In-plane cyclic pseudo-static tests were then performed on full-scale specimens to investigate the influence of the proposed reinforcement system on the lateral in-plane response of the walls, compared to their unreinforced conditions. The main parameters which characterized the cyclic behaviour of the masonry piers, *i.e.* elastic stiffness, lateral strength and displacement capacity, were analysed in relation to the achieved damage mechanism. The numerical study of the research consisted of a series of parametric non-linear analyses on advanced discontinuous models based on the Distinct Element Method (DEM). Different wall dimensions, vertical load levels and boundary conditions, in addition to those tested experimentally, were considered. Moreover, the numerical campaign was also extended varying the bond pattern and the mechanical properties with respect to the experimentally tested solutions. In this paper, the results of the experimental tests on solid brick masonry together with the calibration of the related numerical DEM models were reported.

Keywords: unreinforced masonry walls, masonry seismic strengthening, experimental tests, in-plane cyclic response, non-linear analyses, Distinct Element Method

1. Introduction

The increased interest in improving the energy efficiency of buildings and the seismic performance of structures have recently led to the development of innovative combined reinforcement systems for existing masonry buildings (for example, see [1] and [2]). In this context, Progetto Sisma s.r.l. designed "Resisto 5.9", an external steel modular reinforcement system integrated with a thermal coating made up by insulation panels (*e.g.*, polystyrene, see Fig. 1b). The reinforcement system, reported in Fig. 1a, consists of steel frames, made up of cold formed L-shaped sections and plate elements (obtained from galvanized steel thin sheets), connected to each other by means of steel bolts and to the masonry through chemical anchoring with threaded bars. The modules should be positioned on the external surface of the wall and connected to each other and to the masonry with regular pitch, in order to guarantee the continuity of the reinforcing elements in all directions, as shown in Fig. 1c. More details on the reinforcement system can be found in [3]. Focusing on the structural aspects, the proposed system aims to guarantee an improvement in the connection between orthogonal walls and among walls and horizontal elements, a better redistribution of the seismic actions among the different structural elements, a limitation of the out-of-plane overturning of strengthened walls and an improvement of their in-plane performance.

DOI: https://doi.org/10.5592/CO/2CroCEE.2023.122

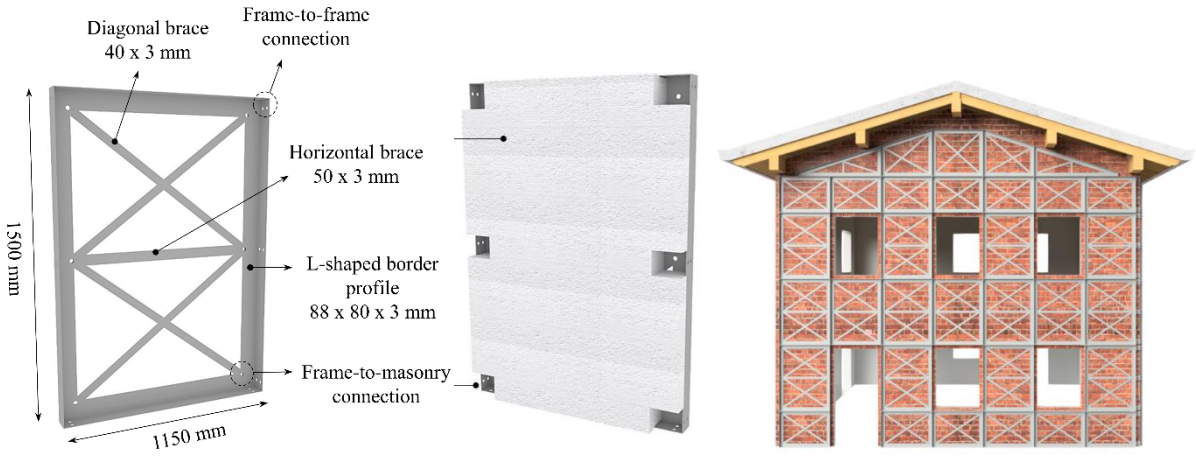

(a) (b) (c)

Figure 1. "Resisto 5.9" system: a) retrofit module details; b) insulation panel; c) example of retrofitted facade.

The study of the in-plane seismic behaviour of the "Resisto 5.9" reinforcement system is the main objective of the experimental and numerical research currently underway at the EUCENTRE Foundation in Pavia. Two different masonry typologies, representing common solutions in Italian existing buildings, have been considered so far in the campaign. This paper focused on a typology made up by solid clay bricks and lime mortar, assembled in "header bond" pattern.

The experimental campaign comprised firstly the complete mechanical characterization of units, mortars, masonry and of the reinforcement system components (*i.e.* steel sections and chemical anchors). Subsequently, the lateral performance of existing masonry piers has been evaluated through cyclic in-plane pseudo-static tests on different sets of full-scale specimens, comparing unreinforced walls with strengthened ones, in order to investigate the effects of the proposed reinforcement system. The cyclic behaviour of the masonry walls was analysed in terms of elastic stiffness, lateral strength, displacement capacity and energy dissipation, associated to the different failure modes.

The experimental results were then supported and extended through an extensive numerical study, which consisted in the development of advanced discontinuum models based on the Distinct Element Method (DEM). Past works in the literature have demonstrated that such models are able to satisfactorily predict the response of unreinforced masonry structures (*e.g.*, [4], [5], [6], [7] and [8]), but the inclusion in DEM framework of possible retrofit solutions represents a topic that has not yet been fully explored. In this study, a numerical procedure to explicitly consider in the models the proposed retrofit system is outlined, and experimental and numerical results are then compared to validate the proposed modelling strategy.

2. Experimental campaign

2.1 Performed tests

The cyclic in-plane pseudo-static shear-compression tests on full-scale masonry specimens were performed at EUCENTRE Foundation, whose experimental laboratory provides a three-dimensional configuration for these type of tests, composed of a strong floor and two orthogonal strong walls. The set-up, reported in Fig. 2a, includes a horizontal actuator, fixed to the strong wall perpendicular to the specimen, that applied the horizontal force, and two vertical actuators, reacting on a steel frame fixed on the strong wall parallel to the specimen, which controlled the applied vertical load and the different boundary conditions. The specimens are built on reinforced concrete (RC) footings, clamped to the strong floor by means of post-tensioned steel bars, while the connection with the actuators is realized through a steel spreader beam connected with the RC beam at the top of the wall. The forces are

Proceedings of the 2nd Croatian Conference on Earthquake Engineering - 2CroCEE
Zagreb, Croatia - March 22 to 24, 2023

DOI: https://doi.org/10.5592/CO/2CroCEE.2023.122

measured by load cells in the different actuators, while the horizontal displacement (δ) of the RC beam at the top of the wall is controlled by an external linear potentiometer. Additional displacement transducers were installed on each wall, in order to evaluate the internal deformations of the masonry pier and, in the case of the strengthened specimens, of the reinforcement system and the relative displacements between them.

The applied testing protocol includes, for all the tests, an initial force-controlled phase followed by displacement-controlled cycles, in which programmed displacements of increasing amplitudes are imposed in both directions, up to the attainment of ultimate conditions of the specimens. At each level of force/displacement amplitude, three cycles were performed, as usually done in similar experimental tests in the past (see [9]). More information about the test set-up, the instrumentation and the testing protocol are reported in [3].

As already stated in the previous section, only solid brick masonry specimens, among the tested ones, are considered in this paper. Specifically, two squat specimens, one unreinforced (Fig. 2b) and the other strengthened (Fig. 2c), with the same mechanical and geometrical properties, were tested. Double-fixed boundary conditions were imposed, along with a realistic value of vertical stress (on this topic, see [10]), in order to achieve a shear failure, according to predictions evaluated with the relevant codified formulations (more information on this issue can be found in [11]). The nominal dimensions and the applied vertical stress level for the considered walls are summarized in Table 1, as well as the already mentioned boundary conditions and failure mode.

Table 1 – Considered masonry specimens subjected to cyclic in-plane tests.

Specimen	**Masonry typology**	**Reinforcement**	***l* (mm)**	***t* (mm)**	***h* (mm)**	**σ_v (MPa)**	**σ_v/fc_m (%)**	**Boundary conditions**	**Failure mode**
UBPS01	Brick	No	2330	250	2435	0.50	7.1	Double fixed	Shear
RBPS01	Brick	Yes	2330	250	2435	0.50	7.1	Double fixed	Shear

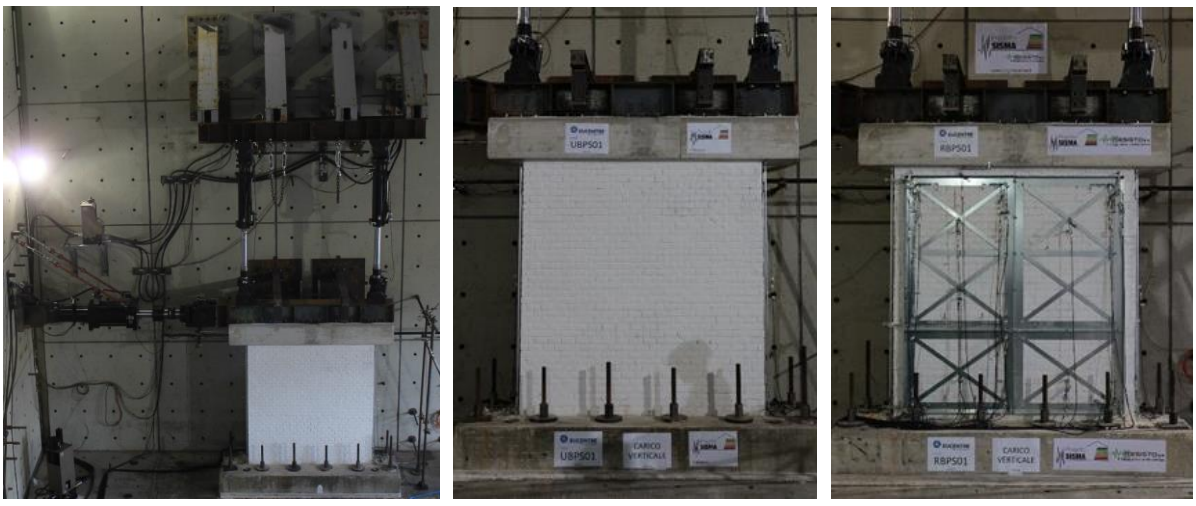

a) b) c)

Figure 2. Experimental in-plane tests: a) set-up; b) unreinforced specimen UBPS01; c) retrofitted specimen RBPS01.

Proceedings of the 2nd Croatian Conference on Earthquake Engineering - 2CroCEE
Zagreb, Croatia - March 22 to 24, 2023

DOI: https://doi.org/10.5592/CO/2CroCEE.2023.122

2.2 Experimental results

The experimental results, in terms of hysteretic curves and related global force-displacement envelopes for the considered tests, are reported in Fig. 3.

As correctly estimated, both specimens, UBPS01 and RBPS01, displayed pure shear failures, with a typical crack pattern characterized by bi-diagonal cracks spreading from corner to corner of the pier. In both cases, cracks were concentrated mostly in the mortar bed- and head-joints with a limited amount in the clay bricks. The shear cracking started developing from a drift ratio ($\theta = \delta/h$) of 0.10% in specimen UBPS01 and 0.15% in the case of specimen RBPS01. Cracks grew in number and width with the increase of the lateral displacement amplitude, progressively reducing the lateral strength and stiffness of the specimens up to their ultimate conditions. Test UBPS01 was stopped at $\theta = 0.25\%$, while RBPS01 at $\theta = 1.00\%$, in both cases to prevent the collapse. Hence, the retrofit system allowed to increase the ultimate displacement capacity of the specimen by about four times, as evident comparing the curves in Fig. 3. The comparison of the results also demonstrates that the initial stiffness was not affected by the presence of the retrofit, as well as the maximum base shear V_{max}, which resulted to be around 240 kN for both specimens. It is evident that, once shear cracks formed, the retrofit contributed in holding the masonry together, significantly reducing and delaying the damage, and thus exploiting the compressive strength of masonry.

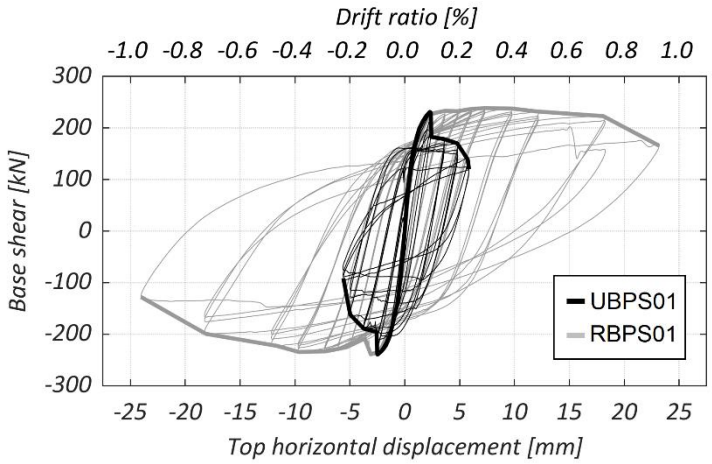

Figure 3. Experimental results, force-displacement curves.

3. Numerical simulation

A simplified micro-modelling strategy, based on DEM, was employed to simulate numerically the in-plane lateral response of the tested specimens. In this type of simplified micro-models, masonry units are expanded up to the half-thickness of the mortar joints (both horizontal and vertical). Bricks are then modelled as continuum blocks, while mortar joints as zero-thickness interface springs. For the complete description of the chosen modelling approach and comprehensive definitions of all the considered parameters it is possible to make reference to [12].

Note that the boundary RC elements, *i.e.* the fully-fixed foundation and the top beam, were modelled as an assembly of linear elastic FD regions (with E = 40000 MPa). Equivalent densities were assigned to the top beam to reproduce the compressive load actually imposed to the specimens.

All the presented numerical models have been implemented within the software 3DEC [13].

3.1 Modelling of the masonry

In this work, masonry units are modelled as deformable blocks, divided into multiple finite-difference (FD) regions, each of them consisting in constant-strain tetrahedral elements. When two blocks are

DOI: https://doi.org/10.5592/CO/2CroCEE.2023.122

detected to be in contact, subcontacts are generated along their interface and zero-thickness springs, characterized by both normal and shear contact stiffnesses (named respectively k_n and k_s) are assigned to these subcontacts. Contact stresses are then calculated in the normal (σ) and shear (τ) directions depending on the related contact stiffnesses. In Fig. 4a a schematic outline of the adopted modelling strategy is reported.

A Coulomb-slip model is employed to represent the contact spring shear behaviour, whereas in the normal direction only a tensile failure is admitted, while no compressive failure is allowed for the joint. In this study, a contact model recently proposed by Pulatsu et al. [7] is employed. This constitutive model allows to account for softening regimes in tension and shear through the definition of fracture energies. Actually, shear (G_s) and tensile ($G_{t,j}$) fracture energy values can be specified to control the contact post-peak behaviour, as shown in Fig. 4c.

The masonry compressive behavior has to be accounted for in the constitutive model defined for masonry units since, as stated previously, no failure in compression is allowed at the interface springs. Therefore, a Mohr-Coulomb plasticity model (MPM) was assigned to the blocks to account for both masonry crushing and unit flexural-splitting failure, as reported in Fig. 4b. It is worth to underline that the proposed strategy combines a discrete modeling approach with masonry units modelled independently, constitutive laws describing their mutual interaction, and a smeared modeling approach to account specifically for masonry crushing and unit failure.

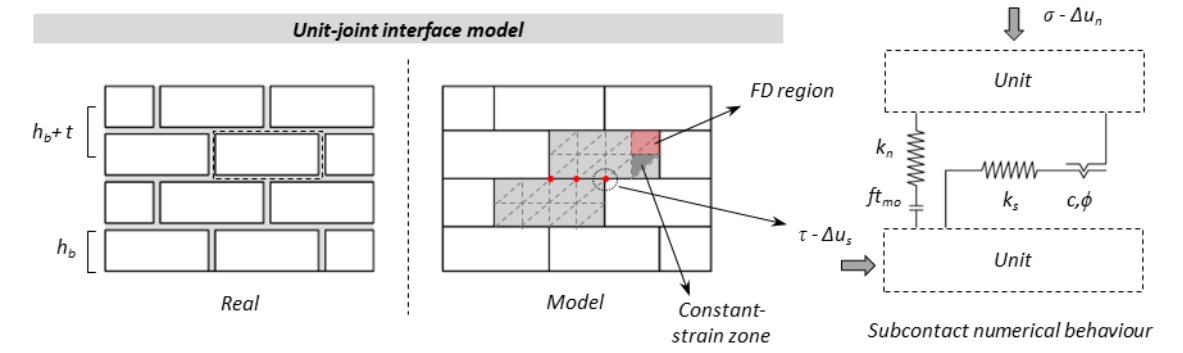

a)

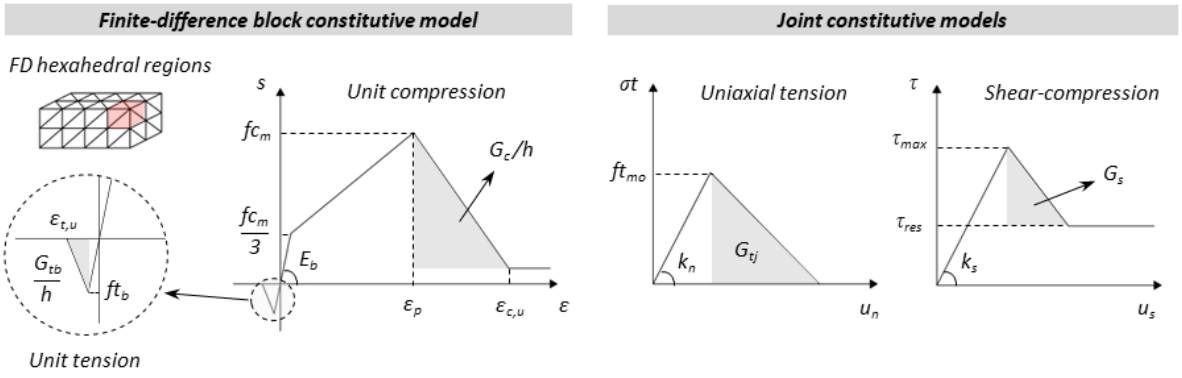

b) c)

Figure 4. Distinct element modelling of masonry: a) unit-joint interface model; b) block constitutive model; c) joint constitutive model.

Before modelling the response of the tested full-scale specimens, the proposed modelling strategy was validated against the characterization tests performed on small-scale assemblages. Specifically, uniaxial compression tests on wallets and shear tests on triplets were reproduced numerically to calibrate the

Proceedings of the 2nd Croatian Conference on Earthquake Engineering - 2CroCEE
Zagreb, Croatia - March 22 to 24, 2023

DOI: https://doi.org/10.5592/CO/2CroCEE.2023.122

required properties, as shown in Fig. 5a,b. Table 2 summarizes all the experimental and inferred properties assigned in the models to blocks and interface springs.

Table 2 – Experimental and inferred material properties employed in the DEM models.

Masonry & Units	E_m [MPa]	G_m [MPa]	fc_m [MPa]	ρ_m [kg/m^3]	fc_b [MPa]	E_b [MPa]	c_b [MPa]	ϕ_b [°]	ft_b [MPa]
	4265[a,b]	1706[a]	7.03[a]	1300[a]	19.22[a]	7207	3.51	0	1.79
Joints	k_n [GPa/m]	k_s [GPa/m]	c [MPa]	ϕ [°]	ft_{mo} [MPa]	G_c [N/m]	G_{tb} [N/m]	G_s [N/m]	G_{tj} [N/m]
	126	50	0.15[a]	31.38[a]	0.05[a]	11248	60	50	10

[a] Value determined through material characterization tests

[b] Evaluated in the direction perpendicular to bed joints as secant value between 10% and 33% of fc_m

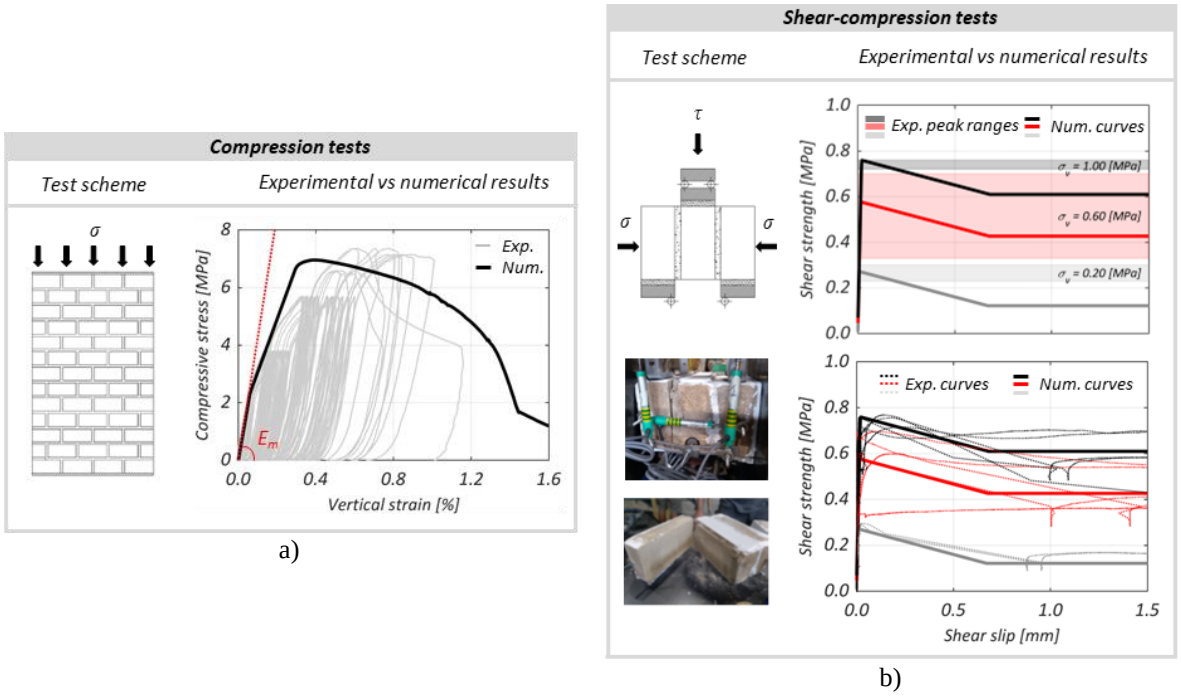

a)

b)

Figure 5. Verification of the modeling strategy with characterization tests on small masonry assemblages: a) vertical compression test; b) shear tests.

3.2 Modelling of the retrofit system

The modular steel frames were numerically reproduced by explicitly modelling each component as a one-dimensional beam finite element (FE) with an isotropic elastic behaviour, with no failure limit. Although this represents a simplified modeling assumption, it was deemed reasonable since experimental evidences demonstrated that the retrofit behaviour was mainly controlled by the failure of the retrofit-to-masonry anchors rather than the attainment of the axial or flexural strength of the steel components (for a complete description, see [14]). FE beams were defined according to the experimental retrofit scheme, connecting the actual positions of the retrofit-to-masonry anchors, as sketched in Fig. 6a. Cross-sectional areas and moments of inertia were then properly assigned, reproducing the actual stiffnesses of the steel members. Moreover, rigid links were inserted in the model in the actual positions to simulate the steel bolts connecting adjacent modular frames (Fig. 6a).

It is important to point out that the thin plate elements employed for the diagonal and horizontal braces (*i.e.* 40x3 and 50x3 mm sections, respectively) experimentally evidenced buckling phenomena that can

Proceedings of the 2nd Croatian Conference on Earthquake Engineering - 2CroCEE
Zagreb, Croatia - March 22 to 24, 2023

DOI: https://doi.org/10.5592/CO/2CroCEE.2023.122

significantly limit their effective compressive strength. For this purpose, an out-of-plane initial deformation was assigned in the numerical models at the mid-length of each diagonal and horizontal brace to account for buckling effects in their compressive behaviour.

As anticipated above, the retrofit system effectiveness was mainly affected by the behaviour of retrofit-to-masonry anchors. Therefore, to simulate correctly the retrofit influence on the pier lateral response, an accurate modelling strategy was required to characterize the connections between the FE beams and the masonry block assembly. In detail, deformable links were defined in correspondence of the actual position of anchors, as shown in Fig. 6a. A shear-yield constitutive model was assigned to each link for the translational in-plane degrees of freedom (directions *x* and *z*, Fig. 6b), while a normal-yield model was assigned for the translational out-of-plane degree of freedom (direction *y*): rotational degrees of freedom were considered as free. The structural link behaviour was calibrated against the results of characterization tests (both shear and pull-out tests) performed on retrofit-to-masonry anchors during the same experimental campaign [3]. A comparison between the experimental shear force-displacement behaviour of anchors and the in-plane numerical model assigned to the structural links is reported in Fig. 6c. Similarly, referring to the experimental results of pull-out tests, a simplified bilinear force-displacement rule was assigned to the out-of-pane translation degree of freedom of the links.

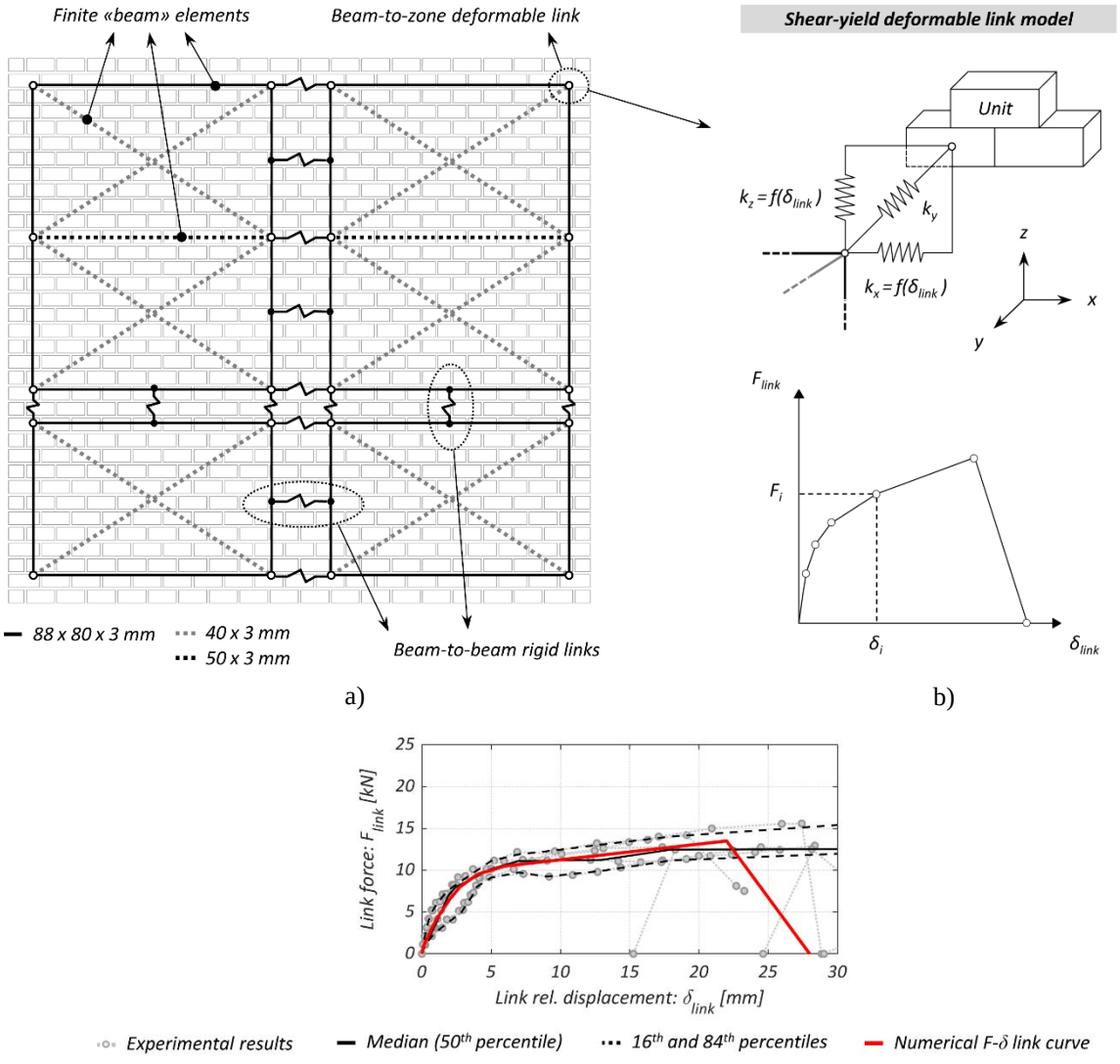

Figure 6. Modelling of the retrofit system: a) retrofit numerical layout; b) retrofit-to-masonry anchors model; c) experimental and numerical anchors shear behaviour along x and z directions.

Proceedings of the 2nd Croatian Conference on Earthquake Engineering - 2CroCEE
Zagreb, Croatia - March 22 to 24, 2023

DOI: https://doi.org/10.5592/CO/2CroCEE.2023.122

3.3 Numerical results

The computational procedure of 3DEC is based on a dynamic time-integration algorithm that solves the equations of motion by an explicit finite difference method. Quasi-static phenomena can be solved with the same algorithm adopting an approach conceptually similar to dynamic relaxation [15]. Specifically, the equations of motion are damped to quickly reach a force equilibrium state through a numerical servo-mechanism, named adaptive global damping [16]. Size, density and time-scaling techniques were also employed according to [6] to obtain an acceptable compromise between the accuracy of results and the computational effort.

The capability of the numerical models to replicate the experimental response was assessed through cyclic and monotonic (*i.e.* pushover) in-plane analyses. It is important to point out that only one cycle for each target displacement has been implemented in cyclic analyses, instead of the three performed in the experimental tests, in order to reduce the computational expense.

The comparison between the numerical and experimental responses of the unreinforced pier (UBPS01) is reported in Fig. 7. Although the numerical model underestimated the initial peak force in both cyclic and monotonic analyses (due to the current inability to capture the tension component of the lateral response of this masonry typology), satisfactory results were obtained in terms of initial stiffness, post-peak response and progressive stiffness and strength degradation (Fig. 7a,b). This latter aspect is particularly relevant, considering that the investigated retrofit solution allowed the wall to reach higher drifts without substantially increasing its lateral strength [14]. Moreover, a good agreement was found between the numerically predicted and the experimental in-plane failure mechanisms, with bi-diagonal stair-stepped cracks adequately simulated by the DEM model crack pattern, as shown in Fig. 7c.

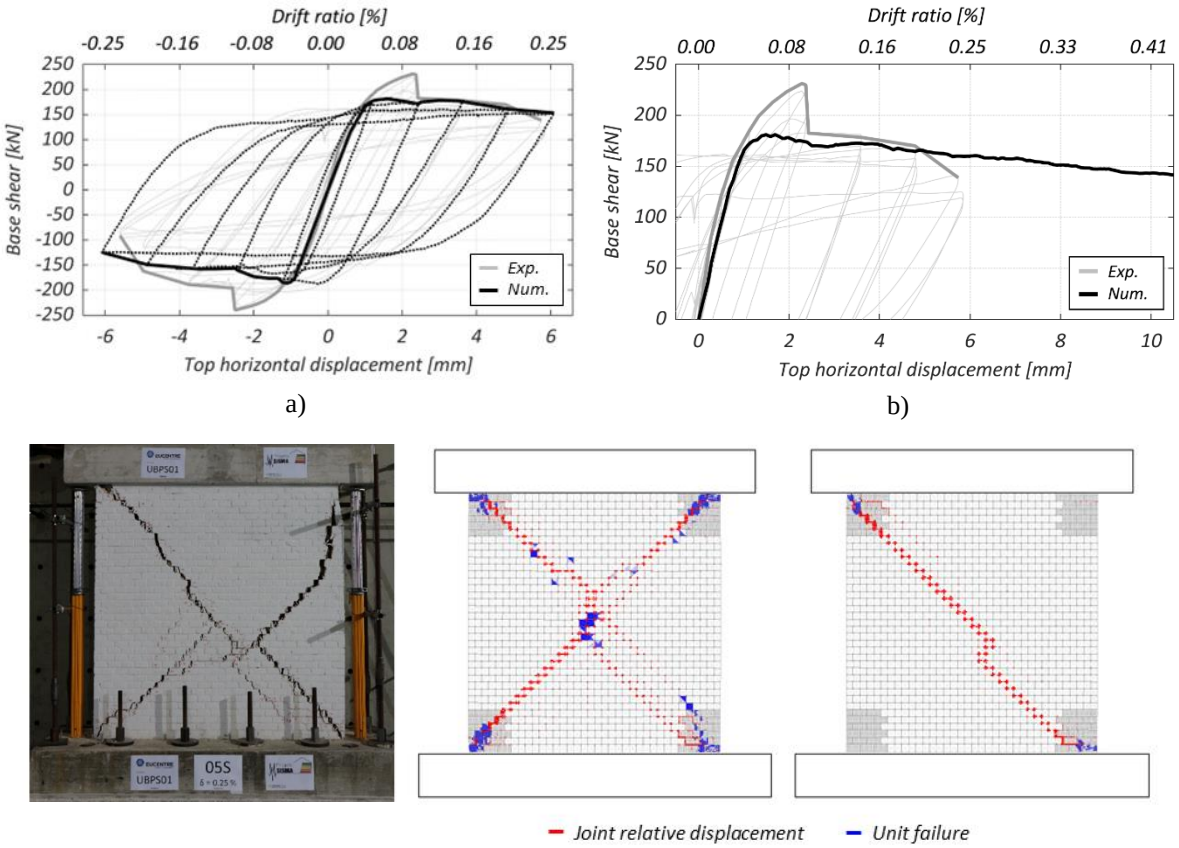

Figure 7. UBPS01 results: a) experimental and numerical hysteresis; b) experimental envelope and numerical pushover; c) experimental and numerical (cyclic and pushover) failure mechanisms.

Proceedings of the 2nd Croatian Conference on Earthquake Engineering - 2CroCEE
Zagreb, Croatia - March 22 to 24, 2023

DOI: https://doi.org/10.5592/CO/2CroCEE.2023.122

The addition of the retrofit frames in the models and the larger target displacements reached in the experimental test of the retrofitted specimen, significantly increased the computational effort resulting in a prohibitive analysis time required for the simulation of the entire experimental cyclic tests. Since the results presented in Fig. 7 demonstrated that monotonic pushover analysis satisfactorily captured the in-plane behaviour of the unreinforced wall, also the numerical performance of the retrofitted one was investigated through this type of analysis. However, the experimental cyclic test was also numerically simulated, but only up to the drift ratio corresponding to the ultimate conditions of the unreinforced specimen (*i.e.* 0.25%).

Fig. 8a compares the numerical and experimental in-plane cyclic responses of the retrofitted pier, simulated, as explained above, only up to the ultimate conditions of the unreinforced specimens, whereas in Fig. 8b, the numerical pushover curve for the retrofitted pier is compared with the experimental envelope. Although the model was not able to capture the specimen maximum lateral strength, as consistently observed for the unreinforced model the numerical response matched satisfactorily the experimental one and reproduced the overall behaviour change caused by the retrofit system. In fact, the comparison between the numerical pushover curves of unreinforced and retrofitted specimens, reported in Fig. 8b, demonstrates that the retrofit system is able to increase the pier ultimate displacement capacity, postponing the strength degradation observed in the unreinforced models, without significantly affecting the pier initial stiffness and strength, as observed experimentally. The ultimate drift of piers subjected to increasing monotonic loads was identified on the pushover curves at a strength reduction of 20% of the maximum base shear. This resulted in an ultimate drift ratio of 0.41% for UBPS01 and of 1.40% for RBPS01.

The retrofit performance can be also appreciated in Fig. 8c (for cyclic analysis) and Fig. 8d (for pushover), with the comparison of the numerical damage patterns at the same level of drift corresponding to the ultimate conditions of URM pier. The damage patterns of the retrofitted wall presented only few diagonal shear cracks with a decreased number of failures in the masonry units, if compared to the unreinforced ones. In Fig. 8c, the cyclic numerical crack pattern of the retrofitted wall is also compared with the corresponding experimental one: the DEM prediction of the effects of the retrofit system on the in-plane behaviour of the specimen closely simulated the reduction of the damage observed in the experimental test. Fig. 8d reports also the damage pattern of the retrofitted piers at its ultimate conditions; the presence of the reinforcement did not alter the diagonal shear failure mechanism exhibited by the unreinforced specimen but, once the mechanism formed, the steel frames restrained the relative displacement of the masonry portions created by the diagonal cracks, reducing the joint opening and spreading the damage over the masonry pier surface.

In Table 3, a comparison between the experimental and numerical values of some of the most relevant parameters of the in-plane lateral response of the investigated specimens is reported, as well as the ratio between retrofitted and unreinforced results. In detail, the maximum absolute base shear (V_{max}), the associated drift ratio (θ_{Vmax}), and the ultimate drift ratio ($\theta_{20\%}$), evaluated at a strength reduction equal to 20% of V_{max}, are considered. Although the numerical ultimate conditions of the retrofitted pier were studied using a monotonic analysis rather than a cyclic one, the experimental response improvement was satisfactorily simulated by the numerical models, especially in terms of displacement capacities, thus confirming the effectiveness of the proposed modelling approach.

Table 3 – Comparison of experimental and numerical retrofit performance.

Specimen	**Experimental (Cyclic)**			**Numerical (Pushover)**		
	V_{max} **[kN]**	θ_{Vmax} **[%]**	$\theta_{20\%}$ **[%]**	V_{max} **[kN]**	θ_{Vmax} **[%]**	$\theta_{20\%}$ **[%]**
UBPS01	239.4	0.08	0.14	184.1	0.06	0.41
RBPS01	238.9	0.10	0.57	200.5	0.20	1.40
R/U ratio [-]	1.00	1.25	4.07	1.09	3.33	3.50

Proceedings of the 2nd Croatian Conference on Earthquake Engineering - 2CroCEE
Zagreb, Croatia - March 22 to 24, 2023

DOI: https://doi.org/10.5592/CO/2CroCEE.2023.122

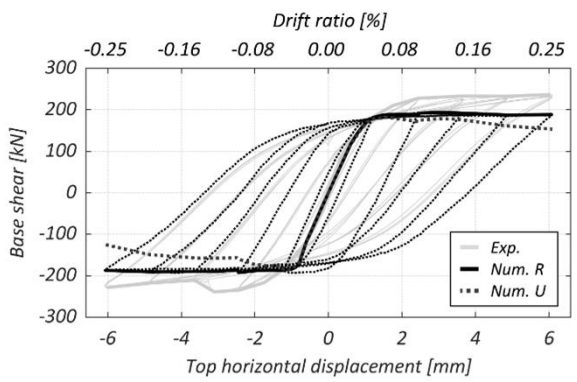

a)

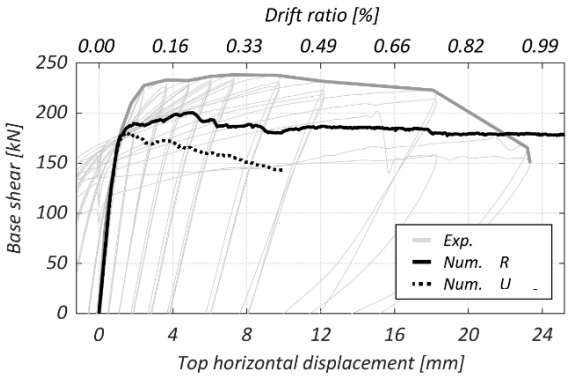

b)

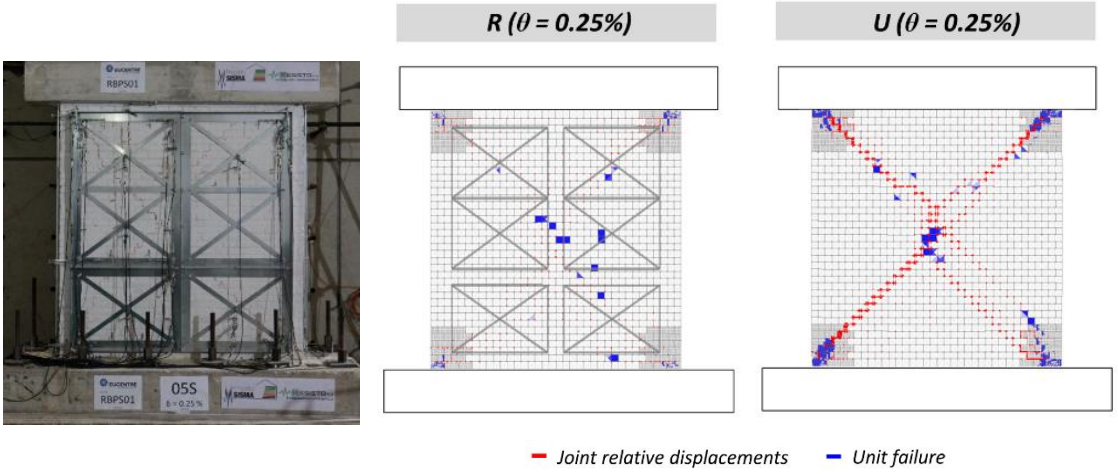

c)

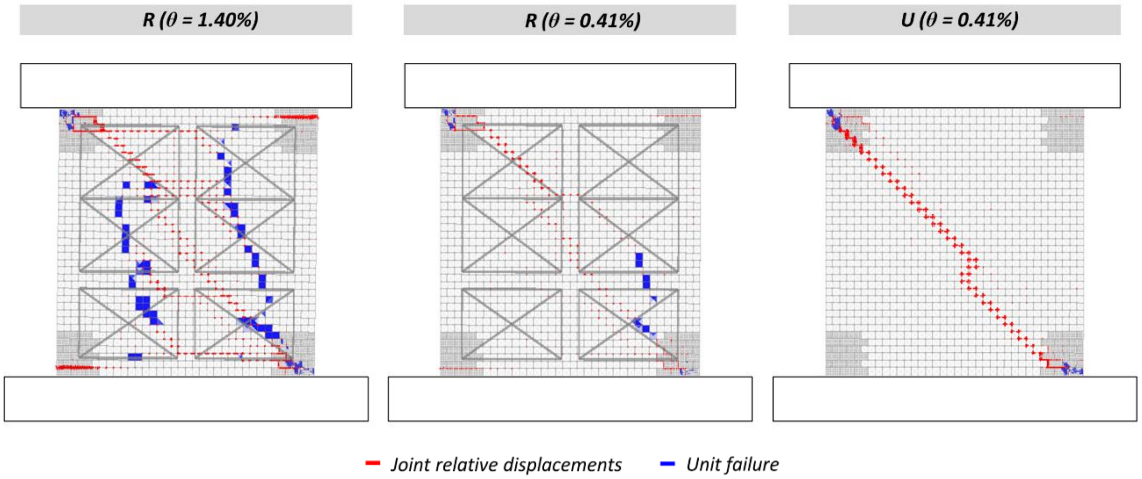

d)

Figure 8. RBPS01 results and comparison with UBPS01: a) experimental and numerical hysteresis; b) experimental envelope and numerical pushover; c) experimental and numerical (cyclic) failure mechanisms; d) numerical (pushover) failure mechanism.

Proceedings of the 2nd Croatian Conference on Earthquake Engineering - 2CroCEE
Zagreb, Croatia - March 22 to 24, 2023

DOI: https://doi.org/10.5592/CO/2CroCEE.2023.122

4. Conclusions

In this paper, an innovative steel strengthening system for the seismic retrofit of unreinforced masonry piers is discussed. The proposed system consists of modular steel frames connected to each other with steel bolts and to the masonry panels through chemical anchors, and aims at enhancing the in-plane and out-plane response of masonry piers. In the experimental campaign, the retrofit was applied to a masonry made of clay bricks arranged in a header bond pattern. Pseudo-static in-plane cyclic tests were performed on both unreinforced and strengthened piers. The tested retrofit solution allowed to increase the displacement capacity of the specimen by approximately four times, while no significant improvement was observed in terms of stiffness and strength.

Advanced discontinuum models based on the Distinct Element Method (DEM) were developed to assess the behaviour of the tested unreinforced and retrofitted piers. A strategy to model unreinforced masonry, simulating all the possible failure mechanisms of masonry components (*i.e.* mortar joint tensile and shear failure, unit flexural and splitting failure, unit crushing) was developed and validated against experimental tests.

A specific modelling strategy to explicitly include the contribution of the investigated steel retrofit solution in DEM framework was then defined. In particular, the retrofit system was modelled as finite-element frames which were connected to the masonry by means of three-dimensional structural links. Despite some differences in terms of maximum lateral strength, the developed model for the strengthening system was able to satisfactorily capture the experimental improvement of the lateral response. Numerical cyclic and pushover analyses demonstrated the capability of the implemented retrofit in delaying the strength degradation and enhancing the pier displacement capacity, without modifying the unreinforced masonry initial failure mechanism, in accordance with the experimental evidences.

In order to generalize the experimental results and to further investigate the effectiveness of the retrofit system, the proposed DEM modelling strategy will be employed to perform a series of parametric analyses aimed at assessing the benefits of the investigated retrofit solution for different pier aspect ratios, vertical loads, boundary conditions, bond patterns, and masonry typologies, as well as retrofit system details.

Acknowledgements

The experimental and numerical research activities, performed at the EUCENTRE Foundation of Pavia in Italy, have been funded by Progetto Sisma s.r.l.. The received financial and technical support is gratefully acknowledged.

References

[1] Guerrini, G., Damiani, N., Miglietta, M., Graziotti, F. (2021): Cyclic response of masonry piers retrofitted with timber frames and boards, *Proceedings of the Institution of Civil Engineers - Structures and Buildings*, 174(5), 372-388, DOI:10.1680/jstbu.19.00134.

[2] Miglietta, M., Damiani, N., Guerrini, G., Graziotti, F. (2021): Full-scale shake-table tests on two unreinforced masonry cavity-wall buildings: effect of an innovative timber retrofit, *Bulletin of Earthquake Engineering*, 19, 2561-2596, DOI:10.1007/s10518-021-01057-5.

[3] Manzini, C., Albanesi, L., Morandi, P. (2022): Studio del comportamento sismico di murature portanti con rivestimento esterno modulare in acciaio - Rapporto Sperimentale, *EUCENTRE Report*. https://www.progettosisma.it/wp-content/uploads/2022/05/2%C2%B0_Sperimentazione_EUCENTRE.pdf

[4] Lemos, J.V. (2007): Discrete element modeling of masonry structures, *International Journal of Architectural Heritage*, 1(2), 190-213. DOI:10.1080/15583050601176868.

[5] Lemos, J.V. (2019): Discrete element modeling of the seismic behavior of masonry construction, *Buildings*, 9(2), 43. DOI:10.3390/buildings9020043.

Proceedings of the 2nd Croatian Conference on Earthquake Engineering - 2CroCEE
Zagreb, Croatia - March 22 to 24, 2023

DOI: https://doi.org/10.5592/CO/2CroCEE.2023.122

[6] Malomo, D., DeJong, M.J., Penna, A. (2019): Distinct element modelling of the in-plane cyclic response of URM walls subjected to shear-compression, *Earthquake Engineering & Structural Dynamics*, 48(12), 1322-1344. DOI: 10.1002/eqe.3178.

[7] Pulatsu, B., Erdogmus, E., Lourenço, P.B., Lemos, J.V., Tuncay, K. (2020): Simulation of the in-plane structural behavior of unreinforced masonry walls and buildings using DEM, *Structures*, 27, 2274-2287. DOI:10.1016/j.istruc.2020.08.026.

[8] Malomo, D., DeJong, M.J. (2021): A Macro-Distinct Element Model (M-DEM) for simulating the in-plane cyclic behavior of URM structures, *Engineering Structures*, 227, 111428. DOI:10.1016/j.engstruct.2020.111428.

[9] Morandi, P., Albanesi, L., Graziotti, F., Li Piani, T., Penna, A., Magenes, G. (2018): Development of a dataset on the in-plane experimental response of URM piers with bricks and blocks, *Construction and Building Materials*, 190, 593-611. DOI:10.1016/j.conbuildmat.2018.09.070.

[10] Morandi, P., Albanesi, L., Magenes, G. (2021): In-plane cyclic response of new URM systems with thin web and shell clay units, *Journal of Earthquake Engineering*, 25(8), 1533-1564. DOI:10.1080/13632469.2019.1586801.

[11] Albanesi, L., Morandi, P. (2021): Lateral resistance of brick masonry walls: a rational application of different strength criteria based on in-plane test results, *International Journal of Architectural Heritage*. DOI:10.1080/15583058.2021.1992533.

[12] Damiani, N., DeJong, M., Albanesi, L., Morandi, P., Penna, A.: Distinct Element Modelling of the in-plane response of a steel-framed retrofit solution for URM structures, *Earthquake Engineering and Structural Dynamics*.

[13] Itasca (2019): 3 Dimensional Distinct Element Code (3DEC): Theory and Background, 7th edition, Itasca Consulting Group, Minneapolis, USA.

[14] Albanesi, L., Manzini, C.F., Morandi, P.: In-plane experimental performance of URM walls strengthened with steel modular framing system integrated with thermal coating, *Engineering Structures*.

[15] Otter, J.R.H. (1966): Dynamic relaxation compared with other iterative finite difference methods, *Nuclear Engineering Design*, 3(1), 183-185. DOI: 10.1016/0029-5493(66)90157-9.

[16] Cundall, P.A. (1982): Adaptive density-scaling for time-explicit calculations, *Proceedings of the 4th International Conference on Numerical Methods in Geomechanics*, Edmonton, Canada, 23-26.